

Fission fragment angular distributions in ${}^6,{}^7\text{Li} + {}^{235,238}\text{U}$ reactions

A. Parihari,¹ S. Santra,^{2,*} A. Pal,² N. L. Singh,¹ K. Mahata,² B. K. Nayak,² R. Tripathi,³ K. Ramachandran,²
P. K. Rath,¹ R. Chakrabarti,² and S. Kailas^{2,4}

¹Department of Physics, The M. S. University of Baroda, Vadodara - 390002, India

²Nuclear Physics Division, Bhabha Atomic Research Centre, Mumbai - 400085, India

³Radio Chemistry Division, Bhabha Atomic Research Centre, Mumbai - 400085, India

⁴UM-DAE Centre for Excellence in Basic Sciences, University of Mumbai, Mumbai 400 098, India

(Received 22 April 2014; revised manuscript received 26 May 2014; published 11 July 2014)

Fission fragment (FF) angular distributions for ${}^6,{}^7\text{Li} + {}^{235,238}\text{U}$ reactions have been measured at energies near and above the Coulomb barrier. The angle integrated fission cross sections for ${}^6\text{Li}$ induced reactions at sub-barrier energies are found to be higher than ${}^7\text{Li}$ induced reactions possibly due to a larger contribution of breakup or transfer induced fission in cases of the former compared to the latter. The FF anisotropies for ${}^6,{}^7\text{Li} + {}^{235}\text{U}$ are found to be slightly smaller than ${}^6,{}^7\text{Li} + {}^{238}\text{U}$, manifesting the effect of target spin. The statistical saddle point model predictions underestimate the measured FF anisotropy for all four systems at measured energies. Anisotropy calculation by entrance channel dependent K -state distribution model and determination of $\langle \ell^2 \rangle$ from continuum discretized coupled channels calculations suggest that the above enhancement in experimental anisotropy is due to a combined effect of entrance channel dependent pre-equilibrium fission and projectile breakup induced fission.

DOI: [10.1103/PhysRevC.90.014603](https://doi.org/10.1103/PhysRevC.90.014603)

PACS number(s): 25.70.Jj, 25.70.De, 25.70.Mn

I. INTRODUCTION

The study of nuclear reaction mechanisms involving weakly bound stable heavy ions has been very interesting due to the observation of many nonconventional behaviors compared to those involving strongly bound projectiles. Fusion suppression at above barrier energies [1–6], absence of threshold anomaly in the real part of the optical potential [7–11], and large production of α particles [12–15] are some of the important features associated with the above reactions. These observations are known to be largely due to the effect of projectile breakup on other channels. Study of fission involving weakly bound projectiles is another avenue. The fission fragment (FF) mass and angular distributions provide a lot of information about the structure and reaction mechanism involving two interacting nuclei [16]. Effect of projectile breakup on different observables like FF angular anisotropy and FF mass distribution has also been discussed in a few studies [17,18]. However, there are very few works in the literature having detailed descriptions on the reaction mechanisms involved in the breakup affected fission observables. Freiesleben *et al.* [17] in their study on ${}^6,{}^7\text{Li} + {}^{232}\text{Th}$, ${}^{238}\text{U}$ have done a systematic work on fission fragment angular distribution and found characteristic differences between ${}^6\text{Li}$ and ${}^7\text{Li}$ induced reactions. They have also mentioned the possibility of projectile breakup and its effect on fission.

Due to a low breakup threshold, the projectile ${}^6\text{Li}$ (${}^7\text{Li}$) can break up into α and $d(t)$ and one of these breakup fragments may get captured by the target forming a composite system which finally fissions into two fragments. Since the breakup fragment carries only a fraction of the total energy of the projectile to the target, the composite system formed by the

capture of one of these fragments [incomplete fusion (ICF)] acquires lower excitation energy compared to the compound nucleus (CN) formed by complete capture of the projectile by the target [i.e., complete fusion (CF)]. The change in the excitation energy may affect FF angular anisotropy because its value depends upon the temperature of the compound nucleus at the saddle point. The anisotropy ‘ A ’ increases with the decrease of the CN temperature ‘ T ’ as $A = 1 + \frac{\langle \ell^2 \rangle \hbar^2}{4I_{\text{eff}} T}$, where $\langle \ell^2 \rangle$ is the mean square angular momentum and I_{eff} is the effective moment of inertia of the CN. Thus a non-negligible contribution from breakup fragment induced fission may lead to a significant change in ‘ T ’ which in turn will change the value of FF angular anisotropy A . Similar effect can also be observed due to transfer induced fission where a few nucleons are first transferred from the projectile to the target nucleus which then breaks into two fission fragments. Distinguishing these two non-CN fission processes experimentally is a difficult task. Thus, any deviation in the behavior of the observed fission fragments from the CN fission could be due to the contamination of breakup and/or transfer induced fissions.

The value of ‘ A ’ may also get modified by any change in the value of the angular momentum ‘ ℓ ’ transferred to the CN. In the measurement of $\langle \ell \rangle$ for the ${}^7\text{Li} + {}^{165}\text{Ho}$ reaction by Tripathi *et al.* [19] it has been shown that the effect of the coupling of the breakup channel is coherent with inelastic or transfer channels. However, with many measurements on the complete fusion cross sections involving weakly bound projectiles providing different conclusions than above, the question of coherence or incoherence of the breakup coupling effect is still unresolved. Since some of the breakup fragments get captured by the target leading to incomplete fusion followed by fission reaction, it contaminates the compound nuclear fission yield. In this case, the inclusive fission data will carry the combined behavior of both CN and non-CN processes. When a breakup fragment

*ssantra@barc.gov.in

is captured by a target nucleus, a different angular momenta is transferred to the target which is expected to change the properties of the composite system and its fission fragments. Alternately, the moments of angular momentum, e.g., $\langle \ell \rangle$ and $\langle \ell^2 \rangle$ of the composite system which are interlinked with its formation cross section and angular momentum transfer to the target, can provide information on different processes leading to fusion followed by fission reaction. So, it would be of interest to determine the $\langle \ell^2 \rangle$ from the measured fission fragment anisotropy and compare them with the ones obtained from coupled channels calculations to investigate the effect of projectile breakup/transfer.

In the present work, we measure the FF angular distribution for ${}^6,7\text{Li}+{}^{235}\text{U}$ systems with a target having a large ground state (g.s.) spin (7/2) to see if their conclusions differ from the study made by Freiesleben *et al.* with the targets (${}^{232}\text{Th}$, ${}^{238}\text{U}$) having zero g.s. spin. We also repeat the measurements of the FF angular distributions for ${}^6,7\text{Li}+{}^{238}\text{U}$ reactions using the present experimental setup for comparing the data for both targets. Thus any systematic error on the data due to the experimental setup between the present reactions with the ${}^{235}\text{U}$ target and the ones from the literature involving the ${}^{238}\text{U}$ target is avoided. The reaction with ${}^{235}\text{U}$ as a target involving a strongly bound projectile is known [20,21] to have different fission anisotropy as compared to the one (${}^{236,238}\text{U}$, ${}^{232}\text{Th}$) having zero g.s. spin. By comparing the data for ${}^6,7\text{Li}+{}^{235}\text{U}$ with ${}^6,7\text{Li}+{}^{238}\text{U}$, it is proposed to investigate if the effect of the target g.s. spin on the FF anisotropy still exists for the reactions involving a weakly bound projectile too, i.e., it is independent of the nature of projectile binding. The FF anisotropy values calculated using different models are compared with the experimental anisotropy to find out the possible factors affecting the observed FF angular distributions.

The paper is organized as follows. Experimental details of the measurements for the FF angular distributions for ${}^6,7\text{Li}+{}^{235,238}\text{U}$ reactions are given in Sec. II. The results for fission cross sections and the FF angular anisotropy along with theoretical calculations are given in Sec. III. Discussion on mean square angular momentum is given in Sec. IV. Finally the results are summarized in Sec. V.

II. MEASUREMENT AND DATA ANALYSIS

The FF angular distribution measurements were carried out using the 14 UD BARC-TIFR pelletron accelerator at Mumbai. Beam (${}^6,7\text{Li}$) energies between 28 to 42 MeV in steps of 2 MeV have been used. Targets of ${}^{235,238}\text{U}$ of thickness $\sim 280 \mu\text{g}/\text{cm}^2$ were prepared by electrodeposition on Al foil ($\sim 800 \mu\text{g}/\text{cm}^2$) as backing. The FFs were detected using five telescopes (ΔE - E) of silicon surface barrier detectors of thickness 12–15 μm for ΔE and 300–1000 μm for E . Two Si surface barrier detectors, one kept at 15° and another kept at 50° were used as monitors for the absolute normalization of fission cross sections. The use of two monitors at two different angles provides a normalization of the data suitable for different beam energies as well as the comparison at the same energies. Contributions of the elastically scattered particles from an Al backing were estimated by independent measurements using a pure Al target of the same thickness as

in the backing. Fission fragment angular distributions for all four systems (${}^6,7\text{Li}+{}^{235,238}\text{U}$) along with the theoretical fits at measured beam energies are shown in Fig. 1. The average interaction energies are smaller by ~ 30 – 40 keV due to energy loss in the half-target thickness.

The measured FF angular distributions in the center-of-mass frame ' $W(\theta)$ ' are fitted with the standard expression for angular distribution [22] as given in the equation

$$W(\theta) \propto \sum_{J=0}^{\infty} (2J+1) T_J \times \sum_{K=-J}^J \frac{(2J+1) |d_{M=0,K}^J(\theta)|^2 e^{-K^2/2K_0^2}}{\sum_{K=-J}^J e^{-K^2/2K_0^2}}. \quad (1)$$

Here $d_{M=0,K}^J(\theta)$ is the rotational wave function [23] and K_0^2 is the variance of the K distributions which is used as a fitting parameter. FF anisotropies, $A = W(180^\circ)/W(90^\circ)$, are obtained from the above fit to the angular distribution.

III. FISSION CROSS SECTIONS AND FF ANGULAR ANISOTROPY

A. Fission cross sections

The total fission cross section (σ_{fiss}) has been obtained by integrating the measured FF angular distribution using the fitted parameters at each beam energy and is shown in Fig. 2. Fission cross sections for all the ${}^6,7\text{Li}+{}^{235,238}\text{U}$ reactions at above-barrier energies are found to be almost the same. However, at sub-barrier energies, the fission cross sections for ${}^6\text{Li}$ induced reactions (represented by hollow and filled circles) are much higher than those for ${}^7\text{Li}$ induced reactions (represented by hollow and filled stars) which are consistent with the observation made by Freiesleben *et al.* [17] for ${}^6,7\text{Li}+{}^{232}\text{Th}$, ${}^{238}\text{U}$ reactions. Since the breakup threshold of ${}^6\text{Li}$ is lower compared to ${}^7\text{Li}$, a larger contribution of breakup induced fission could be the reason for the observation of higher integrated fission cross sections for ${}^6\text{Li}$ induced reactions at these energies. In addition to breakup, there could be some contribution coming from transfer induced fission too. Differences in transfer cross sections involving two different projectiles may also lead to some of the above differences.

From the statistical model calculations using PACE it was observed that the fission probabilities of the CN formed by the above reactions are almost 100%. So, the fusion cross sections calculated by coupled-channels calculations can be assumed to be the same as the complete fusion-fission cross sections for the present reactions and hence they can be compared with the measured fission data. In Fig. 3, the fusion cross sections calculated by the CCDEF code [24] have been compared with the measured fission data for all the systems. The coupling parameters (β_2 and β_4) used for target ground state deformation are taken from the literature [25–27]. For ${}^{238}\text{U}$, $\beta_2 = 0.286$ [25] has been used. An average of β_2 values of ${}^{234}\text{U}$ and ${}^{236}\text{U}$ [25] ($=0.276$) has been used for ${}^{235}\text{U}$. Similar to Refs. [26,27] the $\beta_4 = 0.05$ is used for both the targets. The potential depth was adjusted by a parameter ' dV ' [24,28] in order to change the fusion barrier height so that the calculated fusion reproduces the measured fission excitation function at high energies. The barrier parameters (V_b , r_b , and

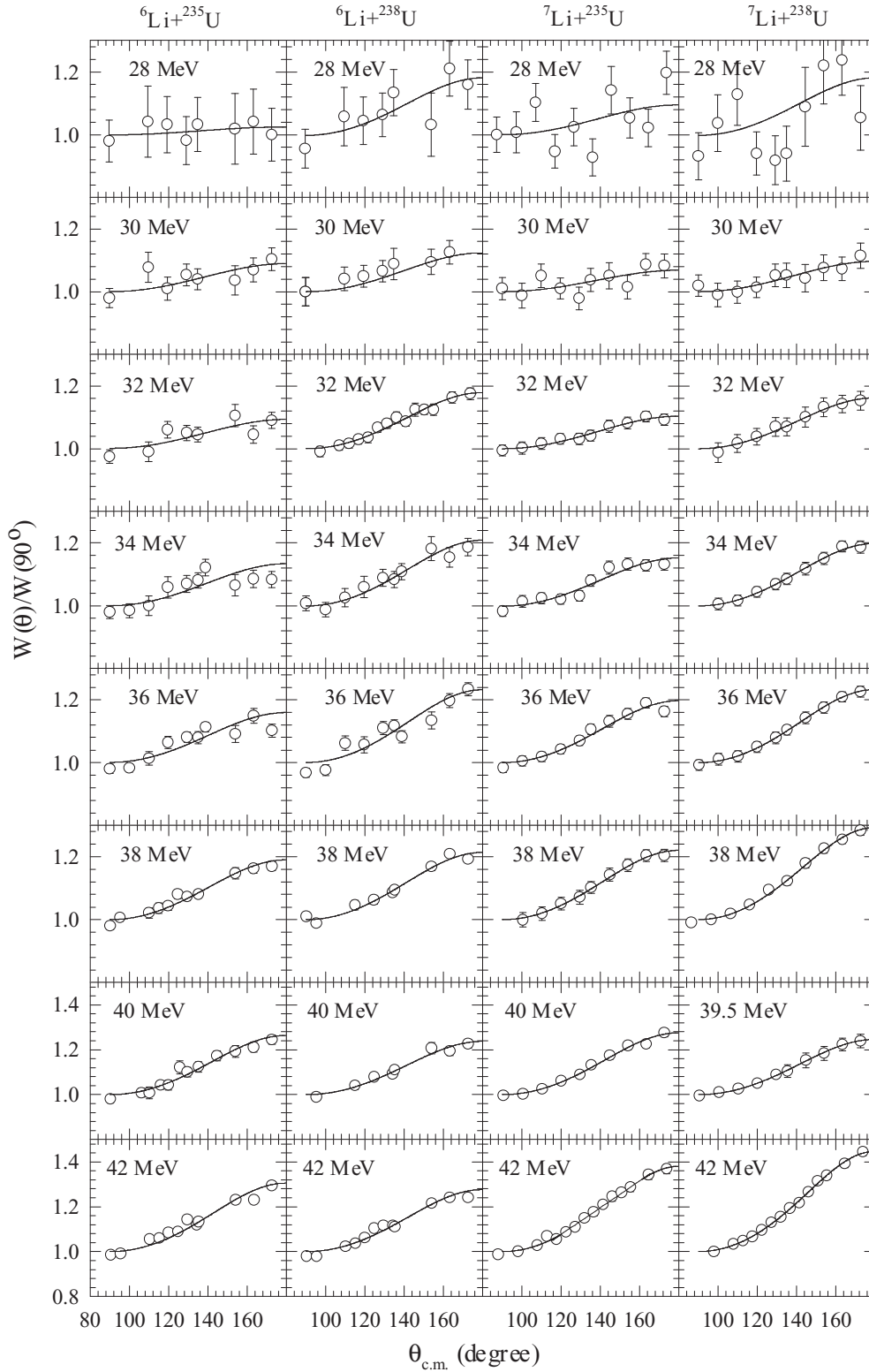


FIG. 1. Fission fragment angular distributions for $^{6,7}\text{Li} + ^{235,238}\text{U}$ systems measured at beam energies in the range of 28–42 MeV. Solid line corresponds to the fit using the standard expression (see text for details).

$\hbar\omega$) used in the above calculations for all four systems are given in Table I. It can be observed from Fig. 3 that the CC predictions at above-barrier energies are close to the measured data for all four reactions. However, at sub-barrier energies,

they are underpredicted for ^6Li induced reactions implying that the relative contribution of breakup/transfer induced fissions are higher for ^6Li compared to those for ^7Li induced reactions.

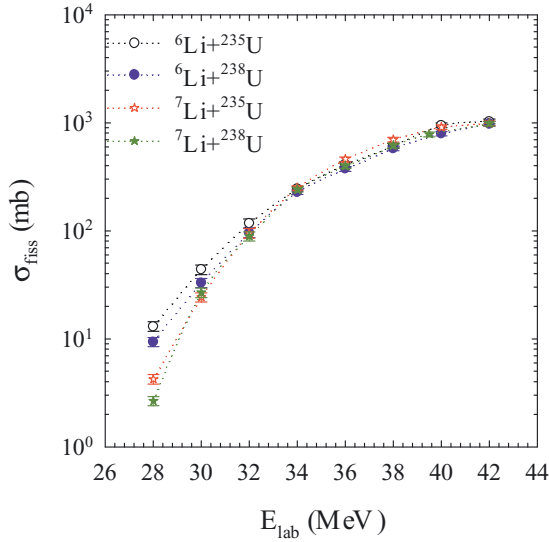


FIG. 2. (Color online) Angle integrated fission excitation functions for ${}^{6,7}\text{Li} + {}^{235,238}\text{U}$ reactions, showing larger cross sections for ${}^6\text{Li}$ induced reactions (compared to ${}^7\text{Li}$) at sub-barrier energies.

B. Fission fragment angular anisotropy

The FF angular anisotropy (A) values are obtained from the measured FF angular distribution data and their corresponding fits for all four reactions at different beam energies and are shown in Fig. 4. It can be observed that the newly measured anisotropy for ${}^{6,7}\text{Li} + {}^{238}\text{U}$ reactions has a nonsmooth energy dependence behavior and is consistent with the previously measured data by Freiesleben *et al.* [17]. However, the absolute values of the present anisotropy values are slightly different from the literature. The present FF angular anisotropy values for the ${}^6\text{Li} + {}^{238}\text{U}$ reaction are found to be slightly larger and

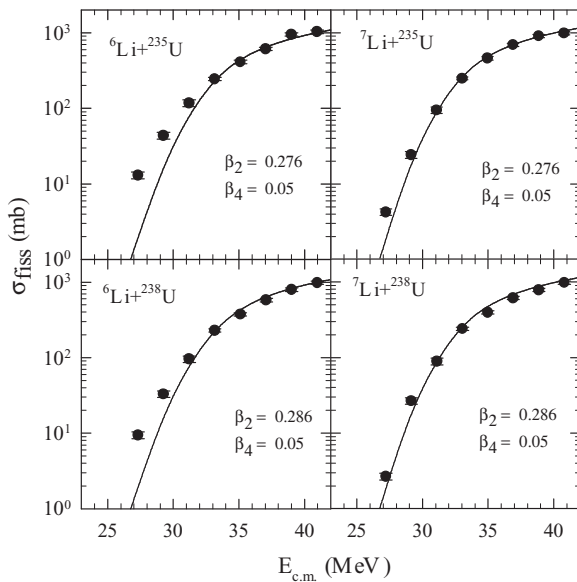


FIG. 3. Fusion cross sections for ${}^{6,7}\text{Li} + {}^{235,238}\text{U}$ reactions calculated by coupled-channels calculations using CCDEF [24] are compared with the measured fission/fusion cross sections.

TABLE I. Fusion barrier parameters (V_b , r_b , and $\hbar\omega$) for ${}^{6,7}\text{Li} + {}^{235,238}\text{U}$ reactions used in CCDEF calculations.

Reaction	V_b (MeV)	r_b (fm)	$\hbar\omega$ (MeV)
${}^6\text{Li} + {}^{235}\text{U}$	32.6	11.31	5.37
${}^7\text{Li} + {}^{235}\text{U}$	32.7	11.26	5.37
${}^6\text{Li} + {}^{238}\text{U}$	32.2	11.45	4.92
${}^7\text{Li} + {}^{238}\text{U}$	32.3	11.40	4.92

for the ${}^7\text{Li} + {}^{238}\text{U}$ reaction they are slightly smaller compared to the ones in the literature. The FF angular anisotropies for the two new systems, i.e., ${}^{6,7}\text{Li} + {}^{235}\text{U}$ are found to have rather smooth behavior as a function of beam energy.

In Fig. 5, the FF anisotropies for the reactions involving the same projectile but two different targets, i.e., ${}^{235,238}\text{U}$, are compared. It can be observed that the anisotropy values for the reactions with ${}^{238}\text{U}$ targets are higher than the ones with ${}^{235}\text{U}$ targets. Such a difference could be attributed to the difference in the target ground-state spin, as all other relevant features (like deformation, mass, charge, etc.) of the two targets are practically the same. FF anisotropy calculated from the entrance channel dependent (ECD) pre-equilibrium model that includes the effect of target spin, described later in a separate subsection, are also plotted as solid and dashed lines corresponding to the reactions involving the ${}^{235}\text{U}$ and ${}^{238}\text{U}$ targets, respectively. The difference in the ECD model calculated anisotropy values for reactions involving

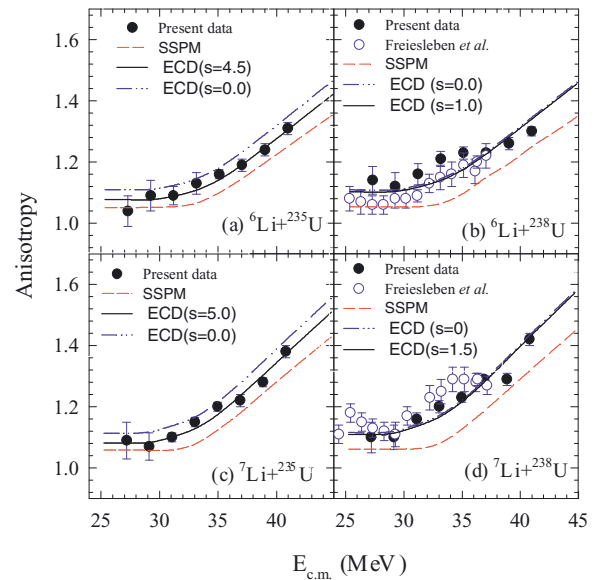


FIG. 4. (Color online) Experimental (filled circles) and calculated fission fragment anisotropies as a function of center of mass energy for (a) ${}^6\text{Li} + {}^{235}\text{U}$, (b) ${}^6\text{Li} + {}^{238}\text{U}$, (c) ${}^7\text{Li} + {}^{235}\text{U}$, and (d) ${}^7\text{Li} + {}^{238}\text{U}$ reactions. Hollow circles represent the data from the literature [17]. Dashed lines correspond to the SSPM calculations. The ECD calculations with and without the spin of the target and projectile are represented by the solid and dash-dot-dot lines, respectively.

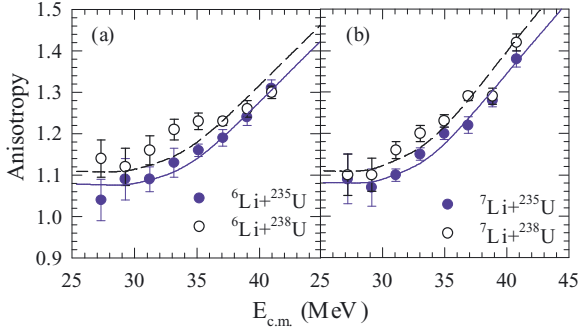


FIG. 5. (Color online) Experimental fission fragment anisotropies as a function of center of mass energy for (a) ${}^6\text{Li} + {}^{235,238}\text{U}$ reactions and (b) ${}^7\text{Li} + {}^{235,238}\text{U}$ reactions showing the effect of target dependence. Solid and dashed lines correspond to the entrance channel dependent (ECD) pre-equilibrium model calculated FF anisotropy for reactions involving the ${}^{235}\text{U}$ and ${}^{238}\text{U}$ targets, respectively.

two different targets shows a similar trend explaining the experimental observation.

C. SSPM calculations

The experimental anisotropies have also been compared with the predictions of the statistical saddle point model (SSPM). Here ‘ A ’ is calculated using the equation “ $A = 1 + \langle l^2 \rangle / 4K_o^2$ ” which is approximated from the expression for fission fragment angular distribution as given in Eq. (1). From the simplified coupled-channels calculations using the CCDEF code mentioned earlier, the values of $\langle l^2 \rangle$ are derived from the fit to σ_{fiss} . Using the ℓ distribution (i.e., σ_ℓ versus ℓ) calculated from the coupled-channels calculations, the average of the square of the angular momentum, i.e., $\langle l^2 \rangle$ for fusion is obtained at each energy. These values of $\langle l^2 \rangle$ are used for anisotropy calculations by the SSPM model.

The variance of the K distributions is $K_o^2 = (I_{\text{eff}}/\hbar^2)T$. Here, I_{eff} is the effective moment of inertia and $T [= \sqrt{E^*/a}]$ with $a = A_{\text{CN}}/10 \text{ MeV}^{-1}$ is the saddle point temperature of the compound nucleus. Excitation energy E^* at the saddle point is given by $E^* = E_{\text{c.m.}} + Q - B_f - E_{\text{rot}} - E_n$, where Q is the Q value for the formation of the compound nucleus. The spin dependent fission barrier ‘ B_f ’, ground-state rotational energy ‘ E_{rot} ’, and effective moment of inertia ‘ I_{eff} ’ are calculated using the Sierk model [29]. ‘ E_n ’ is the average energy removed by the evaporated neutrons from the compound nucleus.

The predicted values of anisotropy by SSPM calculations are shown in Fig. 4 as dashed lines. The SSPM results for all four systems ${}^{6,7}\text{Li} + {}^{235,238}\text{U}$ are smaller compared to the measured anisotropy. However, the difference between theory and experiment for ${}^{6,7}\text{Li} + {}^{238}\text{U}$ systems is larger compared to ${}^{6,7}\text{Li} + {}^{235}\text{U}$ systems. There could be several factors behind the above differences in the anisotropy between theoretical SSPM calculations and experimental data. For example, it is known that a reduction in the variance of the K distribution due to pre-equilibrium fission [30] contribution can increase the value of FF anisotropy, and on the other hand, a large g.s. spin of the target or projectile can reduce the anisotropy

at near- and sub-barrier energies [20,21,31]. In addition, a large contribution of break-up induced fission can lead to a reduction in CN temperature [18] which in turn reduces the value of K_o^2 and hence increases the anisotropy (assuming $\langle l^2 \rangle$ to be similar for both CF and ICF fissions). Therefore the above discrepancy between SSPM calculations and experiment could be due to any of the following effects: (a) the change in the K distributions due to the pre-equilibrium fission contribution which has a dependence on the entrance channel, (b) the difference in the ground-state spin of the targets, and (c) the change in average compound nucleus excitation energy and/or $\langle l^2 \rangle$ due to the break-up induced fission contribution.

D. Entrance channel dependence

To understand the above difference in the FF angular anisotropy between the SSPM and experimental data for all the reactions at different energies, the role of pre-equilibrium fission is investigated to find the entrance channel dependence (ECD) on anisotropy if any. In the pre-equilibrium model, it is assumed that the CN is equilibrated in all degrees of freedom except the K degrees of freedom. At sub-barrier energies the FF anisotropy for several reactions involving deformed heavy targets is found to be much larger compared to the standard SSPM model. This is ascribed to the effect of pre-equilibrium fission [30,32,33]. In addition, there is a strong dependence on the entrance channel ground state spin [20,21,31] as well as projectile-target mass asymmetry, $\alpha_{pt} = [A_t - A_p]/[A_t + A_p]$. Pre-equilibrium effect on the FF anisotropy is supposed to be present for the systems with $\alpha_{pt} < \alpha_{BG}$, where α_{BG} is the Businaro-Gallone critical point of mass asymmetry which is parametrized [34,35] as $\alpha_{BG} = 0$ for $x < x_{BG}$, and $\alpha_{BG} = p\sqrt{\frac{x-x_{BG}}{(x-x_{BG})+q}}$ for $x > x_{BG}$. Here, $p = 1.12$, $q = 0.24$, $x_{BG} = 0.396$ with x being the compound nucleus fissility defined as $x = \frac{Z^2/A}{50.88(Z^2/A)_{\text{crit}}}$ and $(\frac{Z^2}{A})_{\text{crit}} = [1 - 1.78(\frac{N-Z}{A})^2]$.

The value of α_{pt} and α_{BG} for the present reactions are calculated and given in Table II. It can be observed that the value of α_{pt} is larger than the α_{BG} for all the reactions suggesting that the effect of pre-equilibrium fission may be negligible. However, the relation used for calculating α_{BG} is valid only for $\ell = 0$. So, it may be possible that an ℓ dependent α_{BG} can favor some pre-equilibrium fission in addition to CN fission which will lead to a difference between the SSPM result and experimental anisotropy. Besides, the difference in the ground-state target spin in the present systems may provide some explanation to the observed difference between the

TABLE II. Entrance channel mass asymmetry α_{pt} and α_{BG} calculated for ${}^{6,7}\text{Li} + {}^{235,238}\text{U}$ systems using the relations given in Refs. [34,35].

Entrance channel	α_{pt}	α_{BG}
${}^6\text{Li} + {}^{235}\text{U}$	0.950	0.887
${}^7\text{Li} + {}^{235}\text{U}$	0.942	0.886
${}^6\text{Li} + {}^{238}\text{U}$	0.951	0.885
${}^7\text{Li} + {}^{238}\text{U}$	0.943	0.885

reactions having two different targets $^{235,238}\text{U}$ with g.s. spin of $7/2$ and 0 , respectively. Therefore, detailed calculations have been made to investigate the effect of ECD on FF anisotropy using the formalism given in Refs. [20,30,32].

The angular distribution according to the SSPM model is given by Eq. (1). Where $e^{-(K^2/2K_0^2)}$ is the equilibrated K distribution at the saddle point just after the fusion. $A = W(180^\circ)/W(90^\circ)$ gives the anisotropy of the fission fragments. Using the above equation, the anisotropy can be approximated as $A = 1 + \frac{\langle \ell^2 \rangle}{4K_0^2}$.

But according to the ECD K -state distribution model, it is expected that, because of the large entrance channel ground-state spin, the anisotropies for deformed actinide targets around the barrier energies get lowered and approach the values expected from the SSPM calculations. This has been confirmed with the experimental observations made in the anisotropy measured for several systems having large g.s. spin of the target, e.g., $^{10,11}\text{B} + ^{237}\text{Np}$ ($s = \frac{5}{2}$) [31], $^{11}\text{B} + ^{235}\text{U}$ ($s = \frac{7}{2}$) [21], etc. Here, the K distribution gets modified depending on the entrance channel ground-state spin of the target and projectile as given below:

$$F(J, K, K') = \exp\left[\frac{-(K - K')^2}{2\sigma_K^2}\right] \times \exp\left[\frac{-K^2}{2K_0^2}\right],$$

where $K' = J \sin \omega$ and $\sigma_K = qJ\sqrt{T}t$ with t being the Bohr Wheeler fission time and q being a constant obtained from the fit to the experimental data. The entrance channel K -state population for a particular angular momentum value J and ω decides the fusion cross section $\sigma_{fus}(J, \omega)$ for the angular momentum value J at various target projectile orientations ω . Now the modified angular distribution is given by

$$W(\theta) \propto \sum_{J=0}^{J_{\max}} \sum_{M=-S}^S \sum_{\omega} \sigma_{fus}(J, \omega) \times \frac{\sum_{K=-J}^J (2J+1) |d_{M=0, K}^J(\theta)|^2 F(J, K, K')}{\sum_{K=-J}^J F(J, K, K')}.$$

Here $\sigma_{fus}(J, \omega)$ is the orientation dependent partial cross section. We have extracted $\sigma_{fus}(J, \omega)$ from the CCDEF code. Results of the above calculations with (without) g.s. spin of the projectile+target (S) are shown in Fig. 4 as solid (dash-dot-dot) lines. The anisotropy values obtained from the ECD K -state distributions are much higher than the SSPM values (dashed lines) and they reproduce the measured values reasonably well. The parameter ' q ' has been adjusted to 0.3 ($\text{MeV} \times 10^{-21} \text{ s}$) $^{-1/2}$ to reproduce the measured anisotropy data assuming the discrepancy between the SSPM anisotropy and experiment is totally due to pre-equilibrium fission. By comparing the solid and dash-dot-dot lines, one can observe that the effect of the g.s. spin ' s ' on anisotropy is prominent in case of $^{6,7}\text{Li} + ^{235}\text{U}$ as ^{235}U has a large nonzero spin ($s = 7/2$) compared to ^{238}U ($s = 0$).

Although the ECD results reproduce the experimental anisotropy for all the four systems quite well, it is not clear whether the enhancement in anisotropy is only due to the presence of pre-equilibrium fission or projectile breakup/transfer induced fission or due to both. The projectile breakup cross section for the reactions involving $^{6,7}\text{Li}$ projectiles with heavy targets at near barrier energies is known to be substan-

tial [1,13,36–39] which alters the CN formation cross sections. For example, in $^7\text{Li} + ^{159}\text{Tb}$ reactions [37], it is observed that the energy spectrum of the tritons and α particles measured at forward angles show a broad bump at energies corresponding to beam velocity which is a characteristic of breakup mechanism. In this measurement, almost half of the α particles are found to be produced due to breakup fusion in which one of the breakup fragments is captured by the target nucleus. Similarly for the $^6\text{Li} + ^{144}\text{Sm}$ reaction [1], about 30% suppression observed in complete fusion cross section is believed to be due to the presence of same fraction of incomplete fusion cross sections. In the present systems, the exact contribution of the complete and incomplete (breakup/transfer-induced) fusion-fission cross sections at different energies are not yet known. A measurement of fission fragments in coincidence with the breakup fragments with large solid angle coverage can help disentangle the above contributions. Alternately, by coupled-channels calculations including the projectile breakup channels, one can estimate the effect of breakup on $\langle \ell^2 \rangle$ and hence the effect on anisotropy ' A '.

IV. DETERMINATION OF $\langle \ell^2 \rangle$

A. $\langle \ell^2 \rangle$ from anisotropy data

The mean square angular momenta $\langle \ell^2 \rangle$ for $^{6,7}\text{Li} + ^{235,238}\text{U}$ reactions are derived from different methods and compared to each other to get the information on possible effects of projectile breakup or pre-equilibrium fission on FF angular anisotropy. First, the $\langle \ell^2 \rangle$ was obtained from the measured FF anisotropy A_{exp} using the relation $\langle \ell^2 \rangle_{\text{aniso}} = (A_{\text{exp}} - 1)4K_0^2$, where the value of $K_0^2 = (I_{\text{eff}}/\hbar^2)T$, the variance of the K distribution is obtained as explained in Sec. II. The results for the $\langle \ell^2 \rangle_{\text{aniso}}$ obtained from the measured anisotropy A_{exp} using the above relations are shown as hollow circles in Fig. 6. It should be pointed out that the T and I_{eff} used for calculating K_0^2 assume complete fusion-fission.

Extraction of $\langle \ell^2 \rangle$ from anisotropy data and possible corrections due to uncertainty in assuming the K_0^2 for this system involving both complete and incomplete fusion components can be justified as follows. The experimental anisotropy has contributions from ^6Li (complete fusion-fission) and from the fragments α or deuteron (incomplete fusion-fission), and can be written as

$$A_{\text{exp}} = aA_{\text{Li}}^{\text{exp}} + bA_{\text{d}}^{\text{exp}} + cA_{\alpha}^{\text{exp}},$$

where a , b , and c are fractional contributions to the anisotropy from the CF ($^6\text{Li} + ^{238}\text{U}$) reaction and ICF ($\alpha + ^{238}\text{U}$ and $\text{d} + ^{238}\text{U}$) reactions, respectively. As $A = 1 + [\langle \ell^2 \rangle / 4K_0^2]$, the above equation can be simplified as

$$\frac{\langle \ell^2 \rangle_{\text{aniso}}}{K_{\text{eff}}^2} = a \frac{\langle \ell^2 \rangle_{\text{Li}}}{K_{0\text{Li}}^2} + b \frac{\langle \ell^2 \rangle_{\text{d}}}{K_{0\text{d}}^2} + c \frac{\langle \ell^2 \rangle_{\alpha}}{K_{0\alpha}^2}.$$

Itkis *et al.* have found [18] that for energies above 30 MeV or so, the breakup fusion-fission has a value of $\sim 20\%$ of the total fusion-fission and this factor remains constant with energy. These ICF contributions modify the values of effective K_0^2 (i.e., K_{eff}^2) which should be used to obtain the values of $\langle \ell^2 \rangle_{\text{aniso}}$. The values of K_0^2 for individual reactions

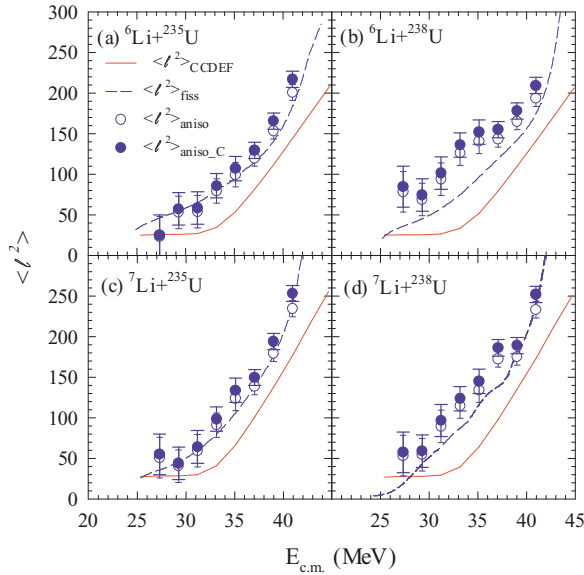


FIG. 6. (Color online) Mean square angular momentum derived from FF anisotropy with and without effective K_0^2 , denoted by $\langle \ell^2 \rangle_{\text{aniso-C}}$ and $\langle \ell^2 \rangle_{\text{aniso}}$, are shown as filled and hollow circles, respectively, for (a) ${}^6\text{Li}+{}^{235}\text{U}$, (b) ${}^6\text{Li}+{}^{238}\text{U}$, (c) ${}^7\text{Li}+{}^{235}\text{U}$, and (d) ${}^7\text{Li}+{}^{238}\text{U}$ reactions. The same obtained from CCDEF calculations ($\langle \ell^2 \rangle_{\text{CCDEF}}$) and from fusion fit by Baba's method ($\langle \ell^2 \rangle_{\text{fiss}}$) [40] are respectively shown as solid and dashed lines.

corresponding to CF and ICF channels have been calculated and shown in Fig. 7. It can be observed that K_0^2 for $\alpha+{}^{238}\text{U}$ and $d+{}^{238}\text{U}$ are similar and roughly ~ 0.7 times that of ${}^6\text{Li}+{}^{238}\text{U}$ at all energies. While saddle point temperatures differ by a factor of two, the effective moment of inertia values will be nearly the same for complete and incomplete fusion-fission. Assuming the anisotropy contribution to be proportional to their cross sections, i.e., $a = 0.8$, $b + c = 0.2$, the above equation can be rewritten as follows:

$$\frac{\langle \ell^2 \rangle_{\text{aniso}}}{K_{\text{eff}}^2} = \frac{0.8\langle \ell^2 \rangle_{\text{Li}} + 1.4(b\langle \ell^2 \rangle_d + c\langle \ell^2 \rangle_\alpha)}{K_{0\text{Li}}^2}.$$

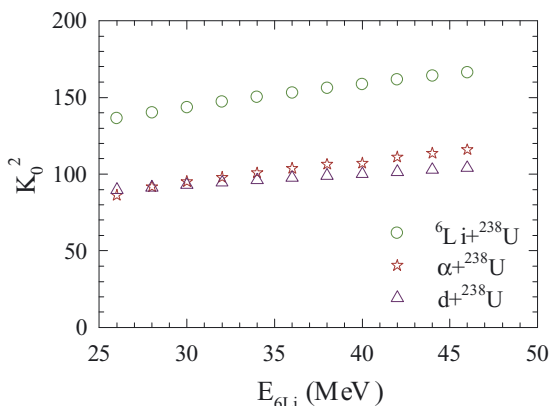


FIG. 7. (Color online) K_0^2 calculated from the Sierk model for ${}^6\text{Li}$, ${}^4\text{He}$, ${}^2\text{H}+{}^{238}\text{U}$ systems.

So, one can use the K_0^2 value for ${}^6\text{Li}$ in extracting the effective $\langle \ell^2 \rangle$ from the fission anisotropy data for comparison with the theoretical calculations. If the $\langle \ell^2 \rangle$ values for the projectile and the fragments are similar, then the extracted effective $\langle \ell^2 \rangle$ will have to be multiplied by a factor 1.08. If the $\langle \ell^2 \rangle$ values for the fragments are significantly smaller than that of the projectile, then the correction to $\langle \ell^2 \rangle$ will be less. In the present work, the extracted $\langle \ell^2 \rangle$ from the anisotropy data (assuming the K_0^2 to be determined for the projectile) shown as hollow circles in Fig. 6 have been corrected upwards by a maximum of 8% and replotted as solid circles in the same figure.

B. $\langle \ell^2 \rangle$ from CC calculation and Baba's method

From the simplified coupled-channels calculations using CCDEF as explained earlier in Sec. III, the ℓ distributions are obtained using whichever values for $\langle \ell^2 \rangle_{\text{CC}}$ are calculated. The results are plotted as solid lines in Fig. 6. It can be observed that the $\langle \ell^2 \rangle_{\text{aniso}}$ derived from the experimental anisotropy for all the systems are on an average higher than the ones calculated from CC calculations. It may indicate that the above difference between $\langle \ell^2 \rangle_{\text{aniso}}$ and $\langle \ell^2 \rangle_{\text{CC}}$ may be due to the effect of additional breakup or transfer channels which are not included in the CC calculations. So, the effect of breakup coupling on $\langle \ell^2 \rangle_{\text{CC}}$ needs to be further investigated.

In a third method, following the prescription by Baba [40], $\langle \ell^2 \rangle_{\text{fiss}}$ is obtained from the measured fission excitation function $\sigma(E)$ using the expression

$$\langle \ell^2 \rangle(E) = \frac{1}{\beta E \sigma(E)} \int_{-\infty}^E \sigma(E') E' dE',$$

where $\beta = \hbar^2/2\mu R_b^2$ with μ being the reduced mass. R_b is the barrier radius obtained by adding the Akyuz-Winther nuclear potential and Coulomb potential for projectile+target nuclei. The results for $\langle \ell^2 \rangle_{\text{fiss}}$ shown by dashed lines are reasonably close to the values of $\langle \ell^2 \rangle_{\text{aniso}}$ for ${}^6,7\text{Li}+{}^{235}\text{U}$ and are slightly underestimated for ${}^6,7\text{Li}+{}^{238}\text{U}$. It may be mentioned that the values of μ and R_b calculated above correspond to complete fusion only.

C. Effect of breakup on $\langle \ell^2 \rangle$

In order to investigate the effect of breakup coupling on $\langle \ell^2 \rangle$ the continuum discretized coupled channels (CDCC) method is employed to include the unbound excitations (breakup) of the projectiles in the couplings using the code FRESKO[41]. The projectile ${}^6\text{Li}$ (${}^7\text{Li}$) is considered to be the cluster of $\alpha + d$ ($\alpha + t$) in bound as well as continuum states. Breakup is assumed to occur via inelastic excitations due to nuclear as well as Coulomb interactions of the projectile with the target. In the continuum, the inelastic excitations up to 8 MeV and α - d (α - t) relative angular momenta up to $L = 2$ ($L = 3$) are included in the couplings. The continuum is discretized into small bins of equal momentum space ($dk \sim 0.14 \text{ fm}^{-1}$). Bin sizes around the resonant states are kept much smaller depending upon the resonance widths.

The projectile-target interaction potentials ($V_{\text{Li}+U}$) are obtained by cluster folding [42] the two fragment-target

TABLE III. Fragment-target potentials used for FRESKO calculations.

Fragment + target	V_0 MeV	r_0 fm	a_0 fm	W MeV	r_w fm	a_w fm	r_c fm
$\alpha + {}^{238}\text{U}$	90.0	1.361	0.578	20.0	1.0	0.4	1.3
$d + {}^{238}\text{U}$	85.0	1.150	0.973	20.0	1.0	0.4	1.3
$t + {}^{238}\text{U}$	140.0	1.150	0.973	20.0	1.0	0.4	1.3

potentials ($V_{\alpha+U}$ and $V_{d/t+U}$). Woods-Saxon volume potential parameters used for the fragment-target interactions are given in Table III. The real part of the $V_{\alpha+U}$ potential, with radius (r_0) and diffuseness (a_0) parameters, is to be same as that of the $\alpha + {}^{209}\text{Bi}$ potential at $E_{\text{lab}} = 24.8$ MeV [43]. Similarly, the above parameters for the real part of V_{d+U} are taken to be the same as that of $d + {}^{208}\text{Pb}$ at 12 MeV [44]. The same geometry is used for the real part of the V_{t+U} potential as that of the V_{d+U} potential. However, the depth of the real part (V_0) for the above potentials is suitably normalized to reproduce the overall fusion excitation function for the present reactions. For the imaginary part, with parameters V_w , r_w , and a_w , only short-range potentials are used to simulate the total fusion cross section due to the absorption of the breakup fragments by the target. Binding potentials for ‘ αd ’ and ‘ αt ’ clusters at the ground state and excited states are taken to be the same as given in Ref. [45].

Using the above potentials the detailed CDCC calculations are performed for the present ${}^{6,7}\text{Li} + {}^{235,238}\text{U}$ reactions. The results for total fusion cross sections and mean square angular momenta for ${}^{6,7}\text{Li} + {}^{238}\text{U}$ reactions with (without) breakup coupling are shown as solid (dash-dot-dot) lines in Fig. 8. The experimental fission cross sections for the ${}^6\text{Li} + {}^{235}\text{U}$ (${}^6\text{Li} + {}^{238}\text{U}$) reaction are shown in Fig. 8(a) as filled (hollow) squares and for the ${}^7\text{Li} + {}^{235}\text{U}$ (${}^7\text{Li} + {}^{238}\text{U}$) reaction in Fig. 8(b) as filled (hollow) diamonds. It can be observed that the total fusion obtained from CDCC calculations reasonably reproduce the experimental data. It is also observed that at sub-barrier energies the fusion cross sections are enhanced compared to the no-coupling results.

The mean square angular momenta obtained from experimental FF anisotropy values, i.e., $\langle \ell^2 \rangle_{\text{aniso}}$ have been plotted in Fig. 8(c,d) as hollow circles to compare with the CC results. It can be observed that the values of $\langle \ell^2 \rangle_{\text{coupl}}$ with BU coupling are enhanced compared to the ones without BU coupling, i.e., $\langle \ell^2 \rangle_{\text{uncoupl}}$ for both the reactions, as expected. However, the enhancement in $\langle \ell^2 \rangle$ for the ${}^6\text{Li} + {}^{238}\text{U}$ reaction is larger than that of ${}^7\text{Li} + {}^{238}\text{U}$, manifesting the effect of the breakup threshold. No visible change is observed in the values of $\langle \ell^2 \rangle$ by replacing ${}^{238}\text{U}$ by ${}^{235}\text{U}$ along with associated spin/parities in the CDCC calculations. Hence, the CDCC results for only ${}^{6,7}\text{Li} + {}^{238}\text{U}$ reactions are shown to bring out the effect of breakup and the breakup threshold energy on $\langle \ell^2 \rangle$. The absolute value of $\langle \ell^2 \rangle$ may depend on how the fragment-target potential parameters are chosen, however, the enhancement of $\langle \ell^2 \rangle$ due to breakup is confirmed. Thus, the difference in $\langle \ell^2 \rangle_{\text{aniso}}$ and A_{exp} compared to the ones obtained from SSPM calculations can also be understood in terms of projectile breakup couplings.

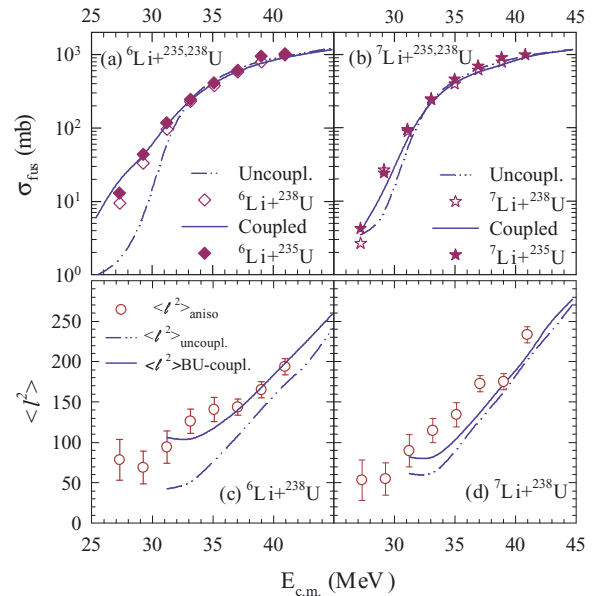


FIG. 8. (Color online) Results of FRESKO calculations with (without) breakup coupling are shown as solid lines (dash-dot-dot lines) for (a,b) total fusion cross sections and (c,d) mean square angular momenta. Experimental angle integrated fission cross sections are shown as symbols for (a) ${}^6\text{Li} + {}^{235,238}\text{U}$ reactions (filled and hollow diamonds) and (b) ${}^7\text{Li} + {}^{235,238}\text{U}$ reactions (filled and hollow stars). Mean square angular momenta derived from FF anisotropy ($\langle \ell^2 \rangle_{\text{aniso}}$) are shown as hollow circles for (c) ${}^6\text{Li} + {}^{238}\text{U}$ and (d) ${}^7\text{Li} + {}^{238}\text{U}$ reactions.

But comparing the experimental anisotropy values involving the same target but different projectiles, i.e., either ${}^{6,7}\text{Li} + {}^{235}\text{U}$ or ${}^{6,7}\text{Li} + {}^{238}\text{U}$, one does not find the expected dependence on the projectile breakup threshold energy. Also, by comparing the anisotropy data for the reactions involving the same projectile but different targets, e.g., comparing ${}^6\text{Li} + {}^{235}\text{U}$ with ${}^6\text{Li} + {}^{238}\text{U}$ one finds that target spin plays an important role as shown in Fig. 5. So, it may be concluded that for the present reactions, the effect of both entrance channel dependent pre-equilibrium fission as well as the projectile breakup contribute to the observed anisotropy and mean square angular momentum.

V. SUMMARY

Fission fragment angular distributions for ${}^{6,7}\text{Li} + {}^{235,238}\text{U}$ reactions are measured at energies around the Coulomb barrier. The angle integrated fission cross sections for ${}^6\text{Li}$ -induced reactions at sub-barrier energies are found to be higher than ${}^7\text{Li}$ -induced reactions with a particular target indicating more contributions from breakup or transfer induced fissions for the former compared to the latter. This can be partially understood in terms of low breakup threshold energy for ${}^6\text{Li}$ that leads to higher breakup cross sections compared to ${}^7\text{Li}$. In addition, there could be contributions coming from transfer induced fissions which are indistinguishable in the present experimental data. Measurements in line with Refs. [36–39] may provide some qualitative idea of these two non-compound-nuclear

fission processes but separating the two contributions may still be difficult as a conventional fragment transfer reaction at optimum Q value gives rise to a similar excitation energy as that of a projectile breakup reaction forming the same outgoing particles. However, Tripathi *et al.* [38] and Udagawa *et al.* [46] have concluded that breakup fusion dominates over transfer.

As observed in Fig. 5, the FF angular anisotropy for reactions involving the ^{235}U target at near-barrier energies is smaller compared to the ones for reactions involving the ^{238}U target with a particular projectile, i.e., ^6Li or ^7Li . This is understood to be due to a larger ground state spin for ^{235}U target. SSPM calculations underestimate the FF angular anisotropy for all four measured reactions. Investigations are made to understand these differences on the basis of an entrance channel dependent K -state distribution as well as projectile breakup coupling. It is found that the measured anisotropy can be understood in terms of ECD K -state distribution and ground-state spin of projectile+target using a q parameter equal to $0.3 (\text{MeV} \times 10^{-21} \text{ s})^{-1/2}$.

Mean square angular momenta of the compound nuclei formed in the above reactions are determined by three different methods: (i) using measured anisotropy data and the simplified equation $\langle \ell^2 \rangle_{\text{aniso}} = 4K_0^2(A_{\text{exp}} - 1)$, (ii) coupled-channels calculations using CCDEF without breakup couplings, and (iii) fitting the measured fission excitation function and applying Baba's formula. It is observed that the $\langle \ell^2 \rangle$ obtained from experimental anisotropy and Baba's method are larger compared to the ones from CC calculations without breakup couplings. In addition to the above, CDCC calculations are also performed to investigate separately the effect of projectile

breakup on a compound nucleus angular momentum and ultimately on FF anisotropy. It is observed that the breakup coupling enhances the values of $\langle \ell^2 \rangle$ which in turn will increase the values of A for all reactions. However, the enhancement is found to be larger for the reactions induced by ^6Li compared to ^7Li , manifesting the effect of breakup threshold.

Thus one can explain the enhancement in measured anisotropy data compared to the SSPM calculations by either the ECD K -state distribution or projectile breakup coupling. However, not all the differences can be understood by a single effect. For example, if breakup is a dominant effect then for ^7Li induced reactions the value of $\langle \ell^2 \rangle$ should be less, K_0^2 should be larger, and A should be smaller compared to that of ^6Li induced reactions. But, with the ratio of the probability of neutron evaporation to fission ' Γ_n/Γ_f ' being larger for the initial compound nucleus with an additional neutron, the anisotropy for $^7\text{Li}+^{235,238}\text{U}$ is expected to be larger compared to $^6\text{Li}+^{235,238}\text{U}$ reactions which is actually observed in the present data. Hence, it can be concluded that the observed differences between the SSPM calculations and the experimental data are due to a combined effect of projectile breakup coupling and entrance channel dependent fission.

ACKNOWLEDGMENTS

The authors would like to thank the pelletron crew for the smooth operation of the accelerator during the experiments. One of the authors (A.P.) acknowledges the financial support from the UGC-DAE CSR, Kolkata Centre for carrying out these investigations.

-
- [1] P. K. Rath, S. Santra, N. L. Singh, R. Tripathi, V. V. Parkar, B. K. Nayak, K. Mahata, R. Palit, S. Kumar, S. Mukherjee *et al.*, *Phys. Rev. C* **79**, 051601(R) (2009).
- [2] C. S. Palshetkar, S. Santra, A. Chatterjee, K. Ramachandran, S. Thakur, S. K. Pandit, K. Mahata, A. Shrivastava, V. V. Parkar, and V. Nanal, *Phys. Rev. C* **82**, 044608 (2010).
- [3] V. V. Parkar, R. Palit, S. K. Sharma, B. S. Naidu, S. Santra, P. K. Joshi, P. K. Rath, K. Mahata, K. Ramachandran, T. Trivedi *et al.*, *Phys. Rev. C* **82**, 054601 (2010).
- [4] M. K. Pradhan, A. Mukherjee, P. Basu, A. Goswami, R. Kshetri, S. Roy, P. R. Chowdhury, M. SahaSarkar, R. Palit, V. V. Parkar *et al.*, *Phys. Rev. C* **83**, 064606 (2011).
- [5] P. K. Rath, S. Santra, N. L. Singh, K. Mahata, R. Palit, B. K. Nayak, K. Ramachandran, V. V. Parkar, R. Tripathi, S. K. Pandit *et al.*, *Nucl. Phys. A* **874**, 14 (2012).
- [6] P. K. Rath, S. Santra, N. L. Singh, B. K. Nayak, K. Mahata, R. Palit, K. Ramachandran, S. K. Pandit, A. Parihari, A. Pal *et al.*, *Phys. Rev. C* **88**, 044617 (2013).
- [7] N. Keeley, S. J. Bennett, N. M. Clarke, B. R. Fulton, G. Tungate, P. V. Drumm, M. A. Nagarajan, and J. S. Lilley, *Nucl. Phys. A* **571**, 326 (1994).
- [8] A. M. M. Maciel, P. R. S. Gomes, J. Lubian, R. M. Anjos, R. Cabezas, G. M. Santos, C. Muri, S. B. Moraes, R. L. Neto, N. Added *et al.*, *Phys. Rev. C* **59**, 2103 (1999).
- [9] C. Signorini, A. Andrighetto, M. Ruan, J. Y. Guo, L. Stroe, F. Soramel, K. E. G. Lobner, L. Muller, D. Pierroutsakou, M. Romoli *et al.*, *Phys. Rev. C* **61**, 061603(R) (2000).
- [10] H. Kumawat, V. Jha, B. J. Roy, V. V. Parkar, S. Santra, V. Kumar, D. Dutta, P. Shukla, L. M. Pant, A. K. Mohanty *et al.*, *Phys. Rev. C* **78**, 044617 (2008).
- [11] S. Santra, S. Kailas, K. Ramachandran, V. V. Parkar, V. Jha, B. J. Roy, and P. Shukla, *Phys. Rev. C* **83**, 034616 (2011).
- [12] G. R. Kelly, N. J. Davis, R. P. Ward, B. R. Fulton, G. Tungate, N. Keeley, K. Rusek, E. E. Bartosz, P. D. Cathers, D. D. Caussyn *et al.*, *Phys. Rev. C* **63**, 024601 (2000).
- [13] S. Santra, V. V. Parkar, K. Ramachandran, U. K. Pal, A. Shrivastava, B. J. Roy, B. K. Nayak, A. Chatterjee, R. K. Choudhury, and S. Kailas, *Phys. Lett. B* **677**, 139 (2009).
- [14] H. Kumawat, V. Jha, V. V. Parkar, B. J. Roy, S. Santra, V. Kumar, D. Dutta, P. Shukla, L. M. Pant, A. K. Mohanty *et al.*, *Phys. Rev. C* **81**, 054601 (2010).
- [15] S. Santra, S. Kailas, V. V. Parkar, K. Ramachandran, V. Jha, A. Chatterjee, P. K. Rath, and A. Parihari, *Phys. Rev. C* **85**, 014612 (2012).
- [16] S. Kailas, *Phys. Rep.* **284**, 381 (1997).
- [17] H. Freiesleben, G. T. Rizzo, and J. R. Huizenga, *Phys. Rev. C* **12**, 42 (1975).

- [18] I. M. Itkis, A. A. Bogachev, A. Y. Chizhov, D. M. Gorodisskiy, M. G. Itkis, G. N. Knyazheva, N. A. Kondratiev, E. M. Kozulin, L. Krupa, S. I. Mulgin *et al.*, *Phys. Lett. B* **640**, 23 (2006).
- [19] V. Tripathi, A. Navin, K. Mahata, K. Ramachandran, A. Chatterjee, and S. Kailas, *Phys. Rev. Lett.* **88**, 172701 (2002).
- [20] J. P. Lestone, A. A. Sonzogni, M. P. Kelly, and R. Vandenbosch, *Phys. Rev. C* **56**, R2907 (1997).
- [21] B. R. Behera, M. Satpathy, S. Jena, S. Kailas, R. G. Thomas, K. Mahata, A. Chatterjee, S. Roy, P. Basu, M. K. Sharan *et al.*, *Phys. Rev. C* **69**, 064603 (2004).
- [22] R. Vandenbosch and J. R. Huizenga, *Nuclear Fission* (Academic Press, New York, 1973).
- [23] A. N. Behkami, *Nucl. Data Tables* **10**, 1 (1971).
- [24] J. Fernandez-Niello, C. H. Dasso, and S. Landowne, *Comp. Phys. Commun.* **54**, 409 (1989).
- [25] S. Raman, C. H. Malarkey, W. T. Milner, C. W. Nester, Jr., and P. H. Stelson, *At. Data Nucl. Data Tables* **36**, 1 (1987).
- [26] Y. Aritomo, K. Hagino, K. Nishio, and S. Chiba, *Phys. Rev. C* **85**, 044614 (2012).
- [27] D. J. Hinde *et al.*, *Phys. Rev. Lett.* **74**, 1295 (1995).
- [28] C. H. Dasso and S. Landowne, *Comp. Phys. Commun.* **46**, 187 (1987).
- [29] A. J. Sierk, *Phys. Rev. C* **33**, 2039 (1986).
- [30] V. S. Ramamurthy and S. S. Kapoor, *Phys. Rev. Lett.* **54**, 178 (1985).
- [31] R. G. Thomas, B. K. Nayak, A. Saxena, D. C. Biswas, L. M. Pant, and R. K. Choudhury, *Phys. Rev. C* **65**, 057601 (2002).
- [32] D. Vorkapic and B. Ivanisevic, *Phys. Rev. C* **52**, 1980 (1995).
- [33] B. K. Nayak, R. G. Thomas, R. K. Choudhury, A. Saxena, P. K. Sahu, S. S. Kapoor, R. Varma, and D. Umakanth, *Phys. Rev. C* **62**, 031601(R) (2000).
- [34] U. L. Businaro and S. Gallone, *Nuovo Cimento* **5**, 315 (1957).
- [35] K. T. Davies and A. J. Sierk, *Phys. Rev. C* **31**, 915 (1985).
- [36] C. M. Castaneda, H. A. Smith Jr., P. P. Singh, J. Jastrzebski, and H. Karwowski, *Phys. Lett. B* **77**, 371 (1978).
- [37] H. Utsunomiya, S. Kubono, M. H. Tanaka, M. Sugitani, K. Morita, T. Nomura, and Y. Hamajima, *Phys. Rev. C* **28**, 1975 (1983).
- [38] V. Tripathi, A. Navin, V. Nanal, R. G. Pillay, K. Mahata, K. Ramachandran, A. Shrivastava, A. Chatterjee, and S. Kailas, *Phys. Rev. C* **72**, 017601 (2005).
- [39] A. Shrivastava, A. Navin, A. Lemasson, K. Ramachandran, V. Nanal, M. Rejmund, K. Hagino, T. Ichikawa, S. Bhattacharyya, A. Chatterjee *et al.*, *Phys. Rev. Lett.* **103**, 232702 (2009).
- [40] C. V. K. Baba, *Nucl. Phys. A* **553**, 719 (1993).
- [41] I. J. Thompson, *Comput. Phys. Rep.* **7**, 167 (1988).
- [42] F. G. Perey and G. R. Satchler, *Nucl. Phys. A* **97**, 515 (1967).
- [43] P. Singh, A. Chatterjee, S. K. Gupta, and S. S. Kerekatte, *Phys. Rev. C* **43**, 1867 (1991).
- [44] P. R. Christensen, A. Berinde, I. Neamu, and N. Scintei, *Nucl. Phys. A* **129**, 337 (1969).
- [45] A. Diaz-Torres, I. J. Thompson, and C. Beck, *Phys. Rev. C* **68**, 044607 (2003).
- [46] T. Udagawa and T. Tamura, *Phys. Rev. Lett.* **45**, 1311 (1980).